Rutherford Scattering

Parker Lewis
Amadie Wijenarayana
Ohio University
Department of Physics and Astronomy, Athens, OH, 45701, USA

December 1, 2024

Abstract

This lab report is Rutherford's scattering experiment. The lab was done at the Edward's Accelerator on Ohio University Campus. It's an experiment where ${}^{4}_{2}\mathrm{He}^{2+}$ beam impinges/scatters from a composition metal foil. This lab had 3-objectives perform energy calibration, composition confirmation, and theory vs. experiment differential cross section comparison with varying angles. The results were that energy calibration had residuals between $-0.1 < R < 0.1$ Mev, and a residual's plot that can be approximated as a constant line. Composition of the foil had the following gold: $79.3 \pm 1.1\%$, silver: $10.99 \pm 0.65\%$, and copper: $9.7 \pm 1.3\%$. This matches closely to the $80, 10, 10\%$ composition requirements. For theory vs. experiment differential cross section per varying angle curve match closely with exception to $\theta_{Detector} = 40 - 60$ degrees. Also ratio between experiment to theory cross section plot was made for absolute scales of varying angle it had a ratio closely matching around $R_{exp/theory} = 0.7$, which is a decent approximation that experiment and theoretical Rutherford cross sections matched per varying angle [1]. [Counts: 179]

1 Theory/Intro

1.1 Lab Overview/Topics

In this chapter of the lab report, an overview of the lab objectives and tasks will be presented, along with a discussion of the theory underlying the experiment. The class was divided into groups to perform offline analysis for Rutherford scattering data, focusing on either varying energy or varying angle. The general overview is as follows: on the first day, pre-run measurements of known quantities required for offline analysis were performed. On the second day, data collection for Rutherford scattering at varying angles was conducted. On the final day, data collection focused on varying energy[1]. The concluding step involved offline analysis, including energy calibration, composition confirmation, and comparison between theoretical and experimental results. More detailed explanations of these steps will be provided in the experimental and analysis chapters.The

remainder of this section will establish the theoretical foundation of Rutherford Scattering. Topics covered include an explanation of what a scattering experiment entails, the significance of impact parameters and scattering angles, the concept of a solid angle, and an introduction to the differential cross-section. A brief discussion of classical and quantum scattering will also be provided, particularly focusing on how Rutherford's cross-section can be derived from these perspectives. The chapter will conclude with a concise derivation and discussion of the transformation from the center-of-mass (CM) frame to the laboratory (Lab) frame. Finally, the physics of the gold foil experiment will be addressed, tying back to the overarching ideas and objectives of the lab. [Counts: 241]

1.2 Differential Cross Section

Before we go into what a differential cross section is lets start with defining what a scattering experiment is. A scattering experiment is composed of two objects of interest in the whole system of said experiment the incoming projectile beam and the target apparatus. The projectile beam can be anything you shoot at towards the target but in all but most cases for scattering experiments it will always be composed of subatomic particles like alphas, electrons, any ion type, hadrons, etc. The target can be stationary or moving also this is based on frame of experiment and how its designed as well but will get into that discussion in a little bit. The target is also made of up of groups of subatomic particles like the list discussed above, but for the stationary scattering experiments it's usually nuclei of specific atom species for example a gold nucleus. In this lab the target was combing composition of gold, silver, and copper nuclei that made up the foil and the projectile was a beam of alphas. As a projectile with its line of approach will either hard scatter with a much heavier target which will then change the path of the incident beam of at a certain point the targets induced field (ex. Electromagnetic Repulsion) will eject the incident beam of particles and change its path this is what all scattering experiments are [2]. This is described pictorially by figure 1a. Scattering experiments are done so internal structure of atoms, interactions between projectile/target, and matter confirmation is proven/shown. A scattering process can be described by two quantities the scattering angle and the impact parameter. A scattering angle described by figure 1a can be thought as the intersection of the incident velocity path-line and the scattered velocity path-line. The impact parameter is the perpendicular distance of the axis that goes through the center of the target and the axis of the initial path line. In classical scattering usually the impact parameter and scattering angle are enough to describe the scattering paths of particles, once its in the realm of subatomic processes then the impact parameter becomes a hard quantity to measure. Also, the impact parameter in most cases can be described as $b(\theta)$ and vice versa for scattering angle. The conservation laws of momentum and energy are what can determine the impact parameter in scattering experiments where its warranted. As stated earlier scattering experiments in most cases can't determine the impact parameter but can determine the scattering angle. This leads to a problem to where the experimenter needs the impact parameter to know dynamical information like the size of the target or the strength of the governing field of the target. Lets says we shoot multiple projectiles and have multiple target arrays that can give the experimenter more info about governing interactions. If the experiment is repeated multiple times that gives even more information about target, incident beam and interactions. This is where scattering theory becomes a statistical theory. The projectiles line of approach of whether it can make a hit is uncertain. The scientist can say that probability

of making hit can be determined [2]. Knowing this the governing relation of scattering theory is defined by

$$N_{sc} = N_{inc} \times \sigma \times n_{tar}. \tag{1}$$

The equation goes like this the scattered counts will equal the probability of making a hit given with the product of the incident counts. The probability of making a hit is defined by effective cross section (σ: area of the target) and the target density (n_{tar}: number of targets/area). The next assumption of a scattering experiment is to give a new definition for equation 1, if the (θ, ϕ) directions do matter for the incident and scattered beam paths and to foreshadow this idea is what leads to the differential cross section. To develop this ideas lets start with pre-defining the solid angle. Here's a mathematical analogy lets start with lets go to figure 1d, the left sided image has circle that is sliced based two ray adjacent from each other. This slice creates an angle between the array and the opposite side of the circular slice is the arc length. This is essentially subtends piece of the whole circle. The angle is defines as the arc length per radius of the ray segment. Here's why this analogy is used now assume we have a sphere as shown in the image of the right, lets say we subtend his sphere by assigning the slice of it to look like a cone with a solid angle between two planes of the cone and opposite side is the circular surface area of the cone. This analogy given the effective definition of the solid angle which like the 2-D circle the solid angle is defined as $\Delta\Omega = \frac{A}{r^2}$. The solid angle is essentially then defined as the angle that defines the slice piece of the cone [2]. Solid angle can also be defined in its differential element form like

$$d\Omega = sin(\theta)d\theta d\phi. \tag{2}$$

To get to differential cross section lets take equation 1 in differential from. In this form:

$$N_{sc}(\text{into } d\Omega) = N_{inc} \times d\sigma(\text{into } d\Omega) \times n_{tar} \tag{3}$$

it applies the discussion that the solid angle gives direction for scattered and incident beams and that each scattering event is described by the specific solid angle it does impinge through. The differential cross section is defined as:

$$d\sigma = \frac{d\sigma}{d\Omega}(\theta, \phi)d\Omega. \tag{4}$$

the integration of equation 4 gives the effective area of the target. Combining equation's 4 and 3 give:

$$N_{\text{sc}} = N_{\text{inc}} n_{\text{tar}} \frac{d\sigma}{d\Omega}(\theta, \phi)d\Omega. \tag{5}$$

This relation is what is used directly in this lab and a good way to end the differential cross section discussion. By algebraic manipulation the differential cross section can be defined simply as the number of scattered particles per incident particles, target density, and solid angle of that specific scattering event. A scattering experiment can then be defined by figures 1b and 1c. In those figures an incident beam of projectiles approaches the point of scatter it then subtends the target based on specific solid angle and exits with a different beam path scattered. This section mechanics is what leads to the derivation of the Rutherford's cross section used in this lab. [Counts: 1061]

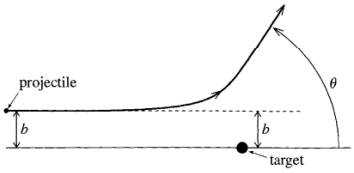

(a) Image that describes a projectile heading towards target and then being scattered by field of the target. Also has description of scattering angle/impact parameter[2].

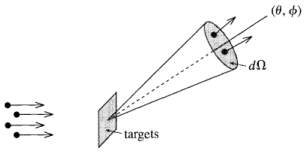

(b) Beam heads towards target and it's scatter orientation (θ, ϕ) is what describes solid angle in scattering experiments [2].

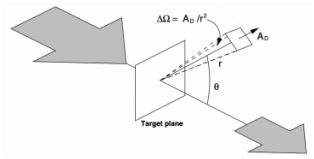

(c) Representation of solid angle subtending from target [3].

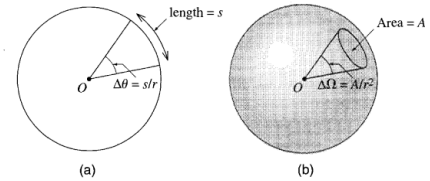

(d) What a solid angle is and how it analogously defined by arc length and angle from 2-D representation [2].

Figure 1: Here is a description that defines concepts like what is a scattering experiment, impact parameter, scattering angle and solid angle.

1.3 Rutherford: Classical Approach

This section will describe how to derive Rutherford's formula using classical mechanics. Only a quick derivation will be developed. In classical mechanics the differential cross section is defined as:

$$\frac{d\sigma}{d\Omega} = \frac{b}{\sin(\theta)} \left| \frac{db}{d\theta} \right|. \tag{6}$$

Based on equation 6, the impact parameter $(b(\theta))$ and the scattering angle (θ) are the ingredients to model differential cross sections using classical mechanics. Lets define the charge of alpha's as charge q, and the gold nucleus as charge Q. The governing force of the nucleus on the alpha particle is

$$F = \frac{kqQ}{r^2}. \tag{7}$$

This is the coulomb force between two charges. The frame of reference is in the CM frame. Figure 2b has a few assumptions that can be taken to get the Rutherford cross section: the alpha has a hyperbolic orbit so that means at the point of closest approach a unit vector **u** can be taken as a symmetric axis which will manipulate to get scattering angle relation. Here are the limiting conditions that help add clarity to the geometry to get scattering angle. At long time assumptions of $(t \to \infty)$ and $(t \to -\infty)$ then the angle between that the unit vector **u** and scattered path segment will be ψ_o. and vice versa for the angle between incident path line and **u** will be This is the coulomb force between two charges. The frame of reference is in the CM frame. Figure 2b has a few assumptions that can be taken to get the Rutherford cross section: the alpha has a hyperbolic orbit

so that means at the point of closest approach a unit vector **u** can be taken as a symmetric axis which will manipulate to get scattering angle relation. Here are the limiting conditions that help add clarity to the geometry to get scattering angle. At long time assumptions of (t $\rightarrow \infty$) and (t $\rightarrow -\infty$) then the angle between that the unit vector **u** and scattered path segment will be ψ_o. and vice versa for the angle between incident path line and **u** will be $-\psi_o$. The geometry for getting the scattering angle is defined as

$$\theta = \pi - 2\psi_o. \tag{8}$$

Next will be to define the impact parameter of the system and relate it to the scattering angle. Using conservation of momentum in the CM frame the change of momentum is defined as

$$\Delta\mathbf{p} = \mathbf{p}' - \mathbf{p} = 0. \tag{9}$$

means that the momentum before and after scattering will have the same magnitude, in this context call it (p). Figure 2a gives a geometrical argument of conservation of momentum that allows to take before and after segments and then enclose them by segment $|\Delta\mathbf{p}|$ which forms a triangle. using known triangle and trig identities then

$$|\Delta\mathbf{p}| = 2\,\mathrm{p}\sin(\frac{\theta}{2}). \tag{10}$$

$|\Delta\mathbf{p}|$ can also be defined by Newtons 2nd Law:

$$|\Delta\mathbf{p}| = \int_{-\infty}^{\infty} F_\mu dt. \tag{11}$$

Using conservation of angular momentum, defining the component of the Coulomb force in the **u** direction, and change of variables to relate to ψ angles give the change of momentum as defined:

$$|\Delta\mathbf{p}| = \frac{2kQqm}{bp}\cos(\frac{\theta}{2}). \tag{12}$$

to get the impact parameter relate equations 12, and 10. The impact parameter is

$$b = \frac{kQq}{mv^2}\cot(\frac{\theta}{2}). \tag{13}$$

To get the Rutherford cross section apply equation 13 to equation 6. Also substitute the mass and velocity products into terms of kinetic energy E. Rutherford's cross section is defined as

$$\frac{d\sigma}{d\Omega} = \left(\frac{kQq}{4E\sin^2\left(\frac{\theta}{2}\right)}\right)^2. \tag{14}$$

This section's derivation is a quick overview from [2]. [Counts: 621]

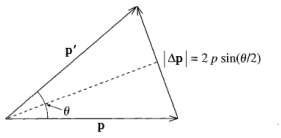

(a) Triangle relation of conservation of momentum used for deriving impact parameter of system [2].

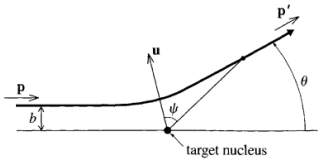

(b) Classical scheme of Rutherford's experiment of alpha particle orbiting a gold nucleus [2].

Figure 2: Illustrations that describe the Rutherford model assuming classical mechanics as an alpha particle approaching gold nucleus and then being ejected by coulomb repulsion following hyperbolic orbit.

1.4 Rutherford: Quantum Approach

In this section the derivation to get the Rutherford cross section is quite tedious so the the things that will be mentioned are the ingredients that lead to same differential cross section using quantum assumptions. Before we begin a quick description of quantum scattering is needed. In quantum scattering the incident projectiles is a wave and essentially the scattering process is the same to where the wave propagates and at a certain point the potential energy function governing the target scatters/distorts the incident wave to not only change direction but have different wave fronts[3]. The Schrodinger equation for center of mass coordinates is what is used to start defining scattering between two quantum bodies. From their, the solutions are defined as superposition of plane waves (incident wave) and spherical waves (scattered wave). For the scattered wave the amplitude of the wave is what relates to the differential cross section in quantum mechanics. It's defined as

$$\frac{d\sigma}{d\Omega} = |f(\theta, \phi)|^2 \,. \tag{15}$$

The quantity $f(\theta, \phi)$ is called the scattering amplitude [3]. An approximation solution of the scattering driven Schrodinger equation can be defined as the Born approximation. Essentially it means that if the target has a weak potential and range then it only does a slight distortion to incident wave. From there the scattering amplitude is defined by

$$f(\theta) = \frac{-2\mu}{\hbar^2 q} \int_0^\infty r' V(r') \sin(qr')\, dr'. \tag{16}$$

- $V(r')$ is the potential of the system.
- r' is the size of the target.
- q is the momentum transfer of before/after collision
- Quantities like: $\hbar$, and μ are known constants.

From everything here apply the Coulomb potential to equations 15 and 16. Then by properly define the momentum transfer of the system, Rutherford cross section is obtained using quantum

mechanics [3]. Figure 3 essentially shows what quantum scattering does. A more detailed derivation is defined from [3]. [Counts: 392]

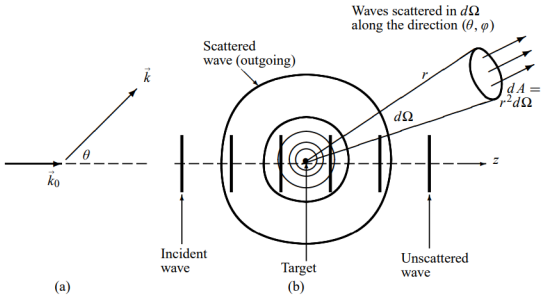

Figure 3: Image that encapsulates the quantum perspective of scattering.

1.5 CM Frame to Lab Frame

In this lab the frame or reference that was used was the lab frame. Here a brief process of how to transform from CM to Lab frame will be shown. In either frame of reference the effective cross sectional area is the same.

$$\sigma_{\text{Lab}} = \sigma_{\text{CM}} \tag{17}$$

In differential form the product of differential cross section and solid angle differential Lab frame will equal the same product in CM frame.

$$\left(\frac{d\sigma}{d\Omega}\right)_{\text{Lab}} d\Omega_{\text{Lab}} = \left(\frac{d\sigma}{d\Omega}\right)_{\text{CM}} d\Omega_{\text{CM}} \tag{18}$$

Using this relation the transformation of the differential cross section of the CM frame to Lab frame is described as

$$\left(\frac{d\sigma}{d\Omega}\right)_{\text{Lab}} = \left(\frac{d\sigma}{d\Omega}\right)_{\text{CM}} \left|\frac{d\cos(\theta)_{\text{CM}}}{d\cos(\theta)_{\text{Lab}}}\right|. \tag{19}$$

The Jacobian term in equation 19 is determined by giving a relation of the scattering angles in the CM/Lab frames. The finals result displayed below is the theoretical Rutherford cross section applied in this lab and its already derived based on applying Jacobian to the CM description of Rutherford cross section and simplifying terms by nuclear physics units.

$$\frac{d\sigma}{d\Omega} = 1.296 \left(\frac{Z_0 Z_1}{E_0}\right)^2 \left[\frac{1}{\sin^4\left(\frac{\theta}{2}\right)} - 2\left(\frac{M_0}{M_1}\right)^2\right] \tag{20}$$

The units used are mb/sr for differential cross section, the mass terms are the alpha and gold masses, the Z-terms are atomic numbers of said species and θ is the scattering angle. E_0 is the incident kinetic energy of the beam[4].[Counts: 228]

1.6 Rutherford Physical Insights

Rutherford's Gold Foil experiment was unique to where it was one of the first experiments that gave the internal structures of the atom. Here is how it went; the alphas came from a lead source would have most go through the gold target and less than others would scatter (figure 4). To be able to detect the alphas zinc sulfide was used to create scintillation effects on the screens to see the patterns of the alphas. The most remarkable conclusion that Rutherford made was that an atom mass is most concentrated which led to discovery of nucleus. [Counts: 97]

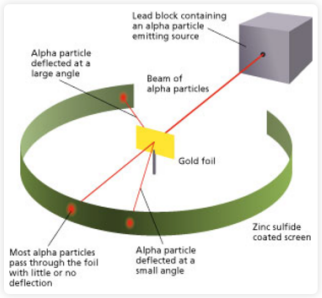

Gold Foil Experiment

Figure 4: The gold foil experiment that describes how to get alpha's, impingement gold target, and showing the scintillation of sulfide screens.

2 Equipment/Procedure

In this section all the components used to run the experiment for each day run will be discussed, along with pre-run measurements, description of trial run days, and how the raw data was displayed. [Counts: 34]

2.1 Equipment Pieces/Beam trial runs

A quick overview of experiment run will be addressed. First thing that was done was to have someone position the detectors at there corresponding angles settings using the angle readout settings in vernier scale outside the chamber. This is shown in figure 5a. Then the operator would setup the energy settings for the alpha beam. The alpha beam is made from a Helium-4 isotope source called the duoplasmatron source [5]. As shown in figure 5b, then the Helium-4 beam goes through sequence of charge stripping/energy gain by the accelerator to become the specified alpha beam [5]. The alpha beam is directed towards the RBS-station to begin the data collecting back scattering and forward scattering collection which is shown in the DAQ system based on figure 5c. Other details to specify are that that charge integrator is what collects and specifies the total charge in the system, the scattering chamber enclose the station to prevent intermolecular reaction of air molecules and alphas, and the two detector is what start the readout processes of taking an electrical signal to a digital pulse in a histogram/spectrum form [1]. [Counts: 185]

- 4.5 MV T-type tandem Pelletron Accelerator.
- Rutherford Back Scattering Station:
  - Beam-line.
  - Fixed Detector, and Movable Detector.
  - Angle Readout.
  - Scattering Chamber.
  - Charge Integrator.
- ADC/DAQ System.
- Operator.

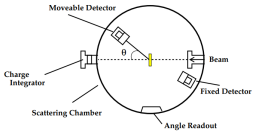

(a) Schematic of the Rutherford chamber for this experiment [1].

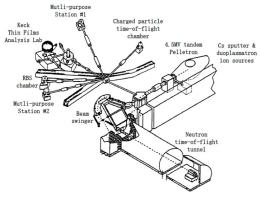

(b) Overview of the accelerator lab at Ohio University [5].

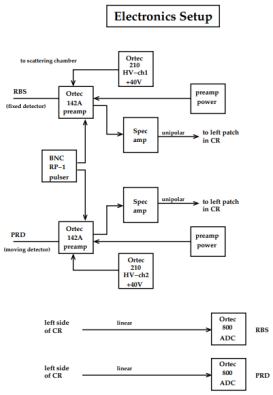

(c) Electrical setup showing how digitized counts are displayed [1].

Figure 5: Main components of this lab using the Edwards Facility at Ohio University to perform Rutherford Scattering experiments.

2.2 Pre-run Measurements

Figure 6, is a table of data collected for solid angle calculations of the detectors. Figure 7 are the are units used for this lab. Experimental differential cross section units are defined by mb/sr.

For the rest of this section the convention of the detectors, data files, are established. For both varying angle/energy data collection days each data set is defined by 4-tag.xy files each ending with a number index. 000# are tag files for varying angle, and 100# for varying energy. the last digit that correspond to 0,1, and 2 and three in sequential order are the xy-files for the PRD, RBS, LT/DT, and BCI [4]. The only data files to use for offline analysis are the ones that correspond to RBS and PRD detectors. [Counts: 124]

Type	Name	Description
RBS	Distance	6.700 ± 0.035 cm
	Diameter	4.01 mm
	Angle (left)	$[225°, 335°]$
	Angle (right)	$[25°, 155°]$
PRD	Distance	6.075 ± 0.035 cm
	Diameter	3.69 mm
	Angle (fixed)	168°

Figure 6: Measurements taken from the RBS/PRD detectors along with defining the angle ranges to use for the experiment [4].

$$1 \text{ barn} = 1 \text{ b} = 10^{-28} \text{ m}^2$$
$$1 \text{ millibarn} = 1 \text{ mb} = 10^{-31} \text{ m}^2$$

Figure 7: Units of area that are used in this lab [1].

2.3 Data Files to Process

Figures 8 and 9 are the data collected and organized from the DAQ system for varying angle and energy data ready to use for offline analysis. Final conventions to establish are, is that DTL are the dead times in percent form for the RBS detector and vice versa for DTR association fro the PRD detector. Other final notes for this section is that the fixed detector (PRD) always was establish as $\theta = 168$ deg, and the movable (RBS) would vary, or be set fixed based on series of data runs. The detector angle is used as the scattering angle in this experiment and essentially if greater than $\theta > 90$ deg, then the target is set to be $\theta = 0$ deg. If $\theta < 90$ deg, then the target is set to be half the detector angle. These are called back scattering and forward scattering processes. [Counts: 148]

Tag	$\theta_{\text{Det.}}$ [deg]	$\theta_{\text{Targ.}}$ [deg]	I [nA]	BCI	DTL [%]	DTR [%]	Time [sec]
20	154.9	0	6	5000	1.0465	1.1628	86
30	60	30	6	5000	1.8391	1.3793	87
40	50	25	6	5000	5.4118	1.2941	85
50	40	20	6	5000	7.6136	1.25	88
60	-45 (215)	-22.5 (337.5)	6	5000	25.053	1.2629	95
70	-55 (305)	-27.5 (332.5)	6	5000	14.286	1.3187	91
80	-65 (295)	-32.5 (327.5)	6	5000	8.4043	1.276	94
90	-90 (270)	-45 (315)	6	5000	3.2673	1.2871	107
100	-90 (270)	-45 (315)	6	5000	3.8043	1.4130	92
110	-115 (245)	0	6	5000	1.5217	1.1957	92
120	-135 (225)	0	6	5000	1.1224	1.1224	98
130*	-35 (325)	-17.5 (342.5)	.6	5000	8.1818	0.56818	88
140*	30	15	.6	5000	10.28670	0.57143	105

(a) Data collection for varying angle data run [4].

Parameter	Value
E_{beam}	2.50 [MeV]
BCI Scale	10^{-8}
θ_{PRD}	168°

(b) Pre-definitions for angle varying data collection [4].

Figure 8: Collection of the tags, energies, scattering angles, BCI, and others for varying angle data collection [4].

Tag	E [MeV]	Θ_{RBS}	Θ_{Targ}	I [nA]	BCI	Scale [10^{-x}]	DTL [%]	DTR [%]	Time [sec]
1010	3.5	50.0 (1)	25.0 (5)	3	5000	8	1.9417	0.72816	206
1020	3.5	155.0 (1)	0.0 (1)	3	5000	8	0.46875	0.72917	192
1030	4.5	155.0 (1)	0.0 (1)	1.5	5000	8	0.34853	0.61662	373
1040	4.5	50.0 (1)	25.0 (1)	1.3	5000	8	0.96685	0.60773	373
1050*	6.5	50.0 (1)	25.0 (1)	1.5	10000	8	1.1679	0.024331	822
1060*	6.5	155.0 (1)	0.0 (1)	1.25	15000	8	0.027027	0.027027	1110

(a) Data collection for varying energy data run [4].

Type	Setting 1	Setting 2
θ_{PRD}	168°	168°
θ_{RBS}	50°	155°
θ_{Targ}	25°	0°

(b) Pre-definitions for energy varying data collection [4].

Figure 9: Collection of the tags, energies, scattering angles, BCI, and others for varying energy data collection [4].

3 Analysis/Results

The offline analysis performed was energy calibration of system, composition confirmation, and theoretical vs. experiment Rutherford. This section will mainly focus on offline analysis on varying angle data. Within each steps, a quick note on uncertainty standards and error propagation will be discussed . [Counts: 47]

3.1 Energy Calibration

For the energy calibration process of this lab, the first thing that was done was to organize the RBS/PRD tag-xy files to make them into a histogram spectra and gaussian fit the peaks. This was achieved by using ROOT as the main tool for processing this step. Figure 10, is an example of what the processing look like. Basically when processing the tags for both run days their is a reference peak that is called the pulsar and it's characteristically the most sharp. The other peaks that are shown are the gold, silver and copper peaks. silver, and copper are less prominent and usually are shown with long run times and higher energy trial runs. gold is the most prominent that is shown in each trial run of this experiment. The gold peaks are what was used for the calibration processing. The data that was extracted from each of the peaks that will be used for the rest of this lab were the mean channel numbers, number of counts, and the corresponding uncertainties that are associated with said data. ROOT as a data analysis tool extracts the mean bin, counts, and uncertainties by applying functional fitting, integral of peaks ranges, and count uncertainties by $\sqrt{N_s}$ statistics. The tags that were used for calibration were the RBS files of tags 20's, 40's, 1010's, 1020's, 1030's, 1040's, 1050's, and 1060's. This included both back scattering and forward scattering processes.

The energy values of the beam spanned from 2.5-6.5 Mev. The next step was to extract the scattered energies from said tags with uncertainties to be able to finalize the calibration plotting. The section below describes the iterative process of how to implement the energy algorithm to get scattered energy values of said peaks and uncertainties. After this step ROOT TGraphErrors plotting classes allowed the implementation of plotting energies in y-axis and mean bins in x-axis. Figure 11, is the resultant linear plot obtained for calibration. ROOT's linear fitting process also allows access to see the linear function to predict the raw data by showing the slope and intercept values and uncertainties. Equation 21, is the linear function that allows the user to go back and forth of mean bin and energies to predict where other peaks will be. To foreshadow this is what is used to find copper and silver peaks. The final step in the calibration step of this part of analysis was to obtain residuals of energies and do a residuals plot of the data. What needs to be seen from this step is to see if the residuals are below 1 Mev, same order of magnitude throughout data points, and to see the trend of residuals per original energies to test if calibration is properly set. The process of how to get the residuals are detailed below. Figure 12, has two main properties the residuals trend is approximately constant, and the residuals range is between $-0.1 < R < 0.1$ Mev. These results show that the calibration of data should be reliable and this result will be useful to reliably find silver and gold peaks which is crucial for next steps. The collection of data for the whole calibration process is displayed by table 1. [Counts: 536]

Peak Processing Examples

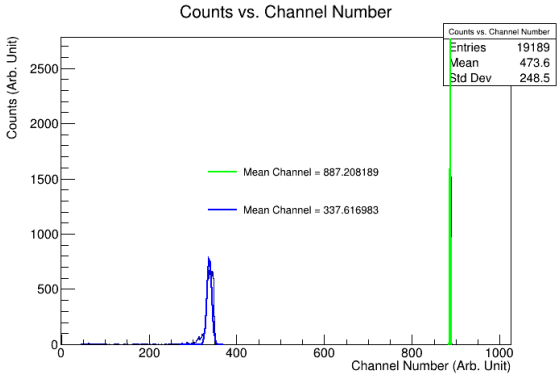

(a) Example of organizing a PRD based tag into a histogram and applying gaussian fitting.

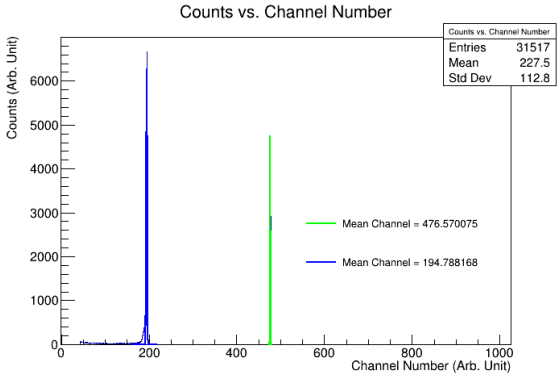

(b) Example of organizing a RBS based tag into a histogram and applying gaussian fitting.

Figure 10: RBS and PRD based tags that are gaussian fitted, and processed. The sharp peaks are the pulsar's shown in distribution, and the peaks with exponential tail are the corresponding gold, silver and copper peaks. Gold is more prominent in these tag files.

Scattered Energy Algorithm

This process describes the algorithm used for energy calculation involving various physical parameters. The process includes energy attenuation, transformation, and uncertainty estimation.

Algorithm Steps

1. Conversion of Degrees to Radians

The angle θ in degrees is converted to radians using the formula:

$$\theta_{\text{radians}} = \theta_{\text{degrees}} \cdot \frac{\pi}{180}.$$

2. Energy Attenuation (E_{att})

The attenuated energy is calculated as:

$$E_{\text{att}} = \text{massStoppingPower} \cdot \left(\frac{\text{molarMass}}{N_A}\right) \cdot \text{compositionFraction} \cdot \text{targetDensity},$$

where:

- massStoppingPower: Energy loss per unit mass (MeV cm^2/g). Stopping power values for helium in gold were obtained from NIST source data base [6].
- molarMass: Molar mass of the target material (gold) (g/mol). The molar masses were obtained by to data bases from IUPAC [7].
- N_A: Avogadro's number (6.022×10^{23}).
- compositionFraction: Fraction of the composition of target. (Initial assumption Gold: 80 %, Silver: 10 %, and Copper: 10%.)
- targetDensity: Density of the target (particles/cm^2).

3. Final Energy After Foil (E_f)

The energy after attenuation is given by:

$$E_f = E_i - E_{\text{att}},$$

where E_i is the initial energy.

4. Average Energy (E_{avg})

The average energy is computed as:

$$E_{\text{avg}} = \frac{E_i + E_f}{2}.$$

5. Kinetic Energy Transformation Factor (K)

The transformation factor K is calculated using the formula:

$$K = \left(\frac{M_o \cos\theta + \sqrt{M_1^2 - (M_o \sin\theta)^2}}{M_o + M_1} \right)^2,$$

where:

- M_o: Mass of the source particle (alphas) (g/mol). The molar mass here was obtained from Pubchem [7]
- M_1: Mass of the target particle (gold, silver, or copper based on context of use.) (g/mol).
- θ: Scattering angle (radians).

6. Scattered Energy ($E_{\mathbf{sc}}$)

The scattered energy is calculated as:

$$E_{\text{sc}} = K \cdot E_{\text{avg}}.$$

7. Uncertainty Calculation

Uncertainty in K

The uncertainty in K is derived using partial derivatives with respect to θ, M_o, and M_1:

$$\Delta K = \sqrt{\left(\frac{\partial K}{\partial \theta}\Delta\theta\right)^2 + \left(\frac{\partial K}{\partial M_o}\Delta M_o\right)^2 + \left(\frac{\partial K}{\partial M_1}\Delta M_1\right)^2}.$$

Uncertainty in $E_{\mathbf{sc}}$

The uncertainty in E_{sc} is given by:

$$\Delta E_{\text{sc}} = E_{\text{sc}} \cdot \sqrt{\left(\frac{\Delta K}{K}\right)^2}.$$

Implementation Notes

- The algorithm loops through various combinations of energy indices and angles. - Intermediate results, such as θ_{radians}, E_{att}, and K, are calculated step by step. - Uncertainties are propagated

systematically using standard error propagation techniques.

Algorithm Conclusion

The described algorithm efficiently calculates scattered energy and its uncertainties for a given set of input parameters. The mathematical formulation ensures accurate and reliable results.

Calibration Plot

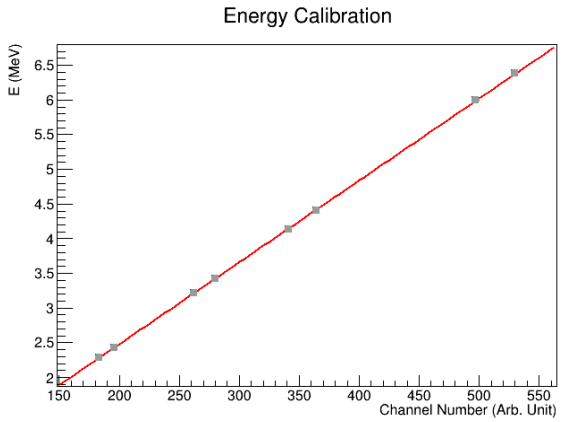

Figure 11: Resultant energy calibration plot with y-axis as energies and x-axis as mean bins.

Calibration Equation

The calibration equation is represented as:

$$E = ax + b, \tag{21}$$

where:

- E: Energy (dependent variable),
- x: Independent variable,
- a: Slope of the line,
- b: Intercept of the line.

Calibration Parameters

The parameters of the calibration equation, adjusted for significant figures, are as follows:

- **Slope (a)**:

$$a = 0.01181 \pm 0.000005(Mev/Bin)$$

- **Intercept (b)**:

$$b = 0.1172 \pm 0.0013(Mev)$$

Residual Algorithm Overview

This algorithm calculates residuals and their uncertainties based on energy calibration data. The key steps involve performing a linear fit, calculating the calibrated energies, and then deriving residuals.

Definitions

- E: Energy (MeV).
- x: Channel number (arb. unit).
- a: Slope of the calibration line.
- b: Intercept of the calibration line.
- σ_a, σ_b: Uncertainties in a and b, respectively.
- $\mathrm{Cov}(a, b)$: Covariance between a and b.
- E_i: Known energy.
- E_{cal}: Calibrated energy.
- Residual: Difference between known and calibrated energy, $R = E_i - E_{\mathrm{cal}}$.

Residual Algorithm

Algorithm 1 Residual Calculation

1: **Input**: Known energies $\{E_i\}$, channel numbers $\{x_i\}$, uncertainties $\{\sigma_{E_i}, \sigma_{x_i}\}$.
2: Perform a linear fit to the data using:

$$E = ax + b$$

to obtain a, b, σ_a, σ_b, and $\mathrm{Cov}(a, b)$.
3: Calculate calibrated energies:

$$E_{\mathrm{cal},i} = ax_i + b$$

4: Calculate calibration errors for each channel:

$$\sigma_{\mathrm{cal},i} = \sqrt{(\sigma_a x_i)^2 + \sigma_b^2 + 2x_i \cdot \mathrm{Cov}(a, b)}$$

5: Compute residuals for each data point:

$$R_i = E_i - E_{\mathrm{cal},i}$$

6: Compute residual uncertainties:

$$\sigma_{R_i} = \sqrt{\sigma_{E_i}^2 + \sigma_{\mathrm{cal},i}^2}$$

7: Output residuals $\{R_i\}$ and uncertainties $\{\sigma_{R_i}\}$.

Residuals Plot

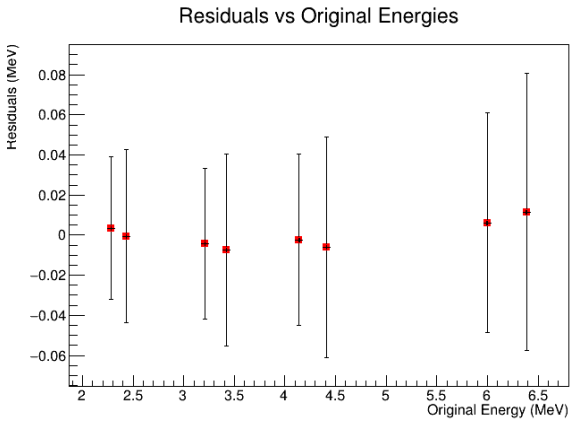

Figure 12: Residuals plot of all the corresponding tags. The trend shown here are residuals approximately constant line, and with $-0.1 < \mathrm{R} < 0.1$ Mev range.

Table of all Calibration Data/Step

Tags Used	Mean Bin	N_s (Counts)	E_{sc} (MeV)	E_{Cal} (MeV)	R (MeV)
tag0021	183.10 ± 0.04	9984 ± 16	2.283 ± 0.001	2.279 ± 0.001	0.004 ± 0.036
tag0041	196.00 ± 0.01	55917 ± 110	2.431 ± 0.001	2.432 ± 0.001	−0.001 ± 0.043
tag1011	280.42 ± 0.01	54386 ± 235	3.421 ± 0.002	3.429 ± 0.001	−0.008 ± 0.048
tag1021	262.46 ± 0.04	4836 ± 72	3.212 ± 0.001	3.217 ± 0.001	−0.005 ± 0.037
tag1031	340.91 ± 0.05	2897 ± 55	4.141 ± 0.001	4.143 ± 0.001	−0.002 ± 0.043
tag1041	364.02 ± 0.02	2381 ± 59	4.410 ± 0.002	4.416 ± 0.001	−0.006 ± 0.055
tag1051	529.78 ± 0.02	3136 ± 66	6.385 ± 0.003	6.373 ± 0.001	0.012 ± 0.069
tag1061	497.24 ± 0.04	4365 ± 67	5.995 ± 0.002	5.989 ± 0.001	0.006 ± 0.055

Table 1: This is all the data obtained from ROOT's fitting processes, developed algorithms, and plotting steps applied for the calibration analysis.

3.2 Composition Confirmation

In this step of the offline analysis the objective here was to re-obtain the composition of the target and prove the 80%, 10%, and 10% composition for gold, silver and copper contributions of the target. Here is a quick overview of how this was achieved; first choose a tag to process. Then the scattered energy algorithm was applied from section 3.1, to obtain the scattered energies of copper, silver and gold of said peak. Then based on tag chosen re-process and fit to get number of signal counts and uncertainties of these peaks. the uncertainties for counts still follow $\sqrt{N_s}$ statistics. Then for the final steps the composition algorithm will be applied to be able to get final compositions for copper, silver and copper in percent form. This section will establish said process for every step, but the crucial equations that are used are equations 20, and 5. These are what build the algorithm. Error propagation and uncertainties discussion will be shown here as well. For composition analysis tag1061 was chosen for this step (figure 13). After applying the composition algorithm below the compositions for gold, silver, and copper were: 79.28 ± 1.12%, 10.99 ± 0.65%, and 9.73 ± 1.30%. The compositions acquired from the algorithm confirmed the initial hypothesis of the makeup of the target. [Counts: 218]

Composition Algorithm

Algorithm Overview/Steps

This document describes the algorithm used to calculate theoretical cross-sections, partial ratios, and compositions for gold, silver, and copper using assumed theoretical Rutherford scattering .

Algorithm 2 Main Algorithm for Composition Calculation

1: **Input:**

- Atomic numbers Z_0, Z_1, masses M_0, M_1, and their uncertainties. Obtained from [7] and [8].
- Experimental counts (N) and their uncertainties ($\sqrt{N}$).
- Initial energy E_0 (MeV) and scattering angle θ (degrees).

2: **Step 1: Calculate Differential Cross-Sections**

$$\frac{d\sigma}{d\Omega} = k \cdot \left(\frac{Z_0 Z_1}{E_0}\right)^2 \cdot \left[\frac{1}{\sin^4(\theta/2)} - 2\left(\frac{M_0}{M_1}\right)^2\right], \tag{22}$$

where:

- $k = 1.296$ (mb MeV^2/sr),
- θ is converted to radians: $\theta_{\text{rad}} = \theta \cdot \frac{\pi}{180}$,
- $\frac{d\sigma}{d\Omega}$ is the differential cross-section (mb/sr).

3: Calculate uncertainty in the cross-section using error propagation:

$$\Delta\left(\frac{d\sigma}{d\Omega}\right) = k \cdot \left(\frac{Z_0 Z_1}{E_0}\right)^2 \cdot \sqrt{\Delta_{\sin}^2 + \Delta_{\text{mass}}^2},$$

where $\Delta_{\sin}$ and Δ_{mass} are derived from uncertainties in $\sin(\theta/2)$, M_0, and M_1.

4: **Step 2: Calculate Partial Ratios**

$$R = \frac{N_1}{N_2} \cdot \frac{\frac{d\sigma_2}{d\Omega}}{\frac{d\sigma_1}{d\Omega}}, \tag{23}$$

with uncertainty:

$$\Delta R = R \cdot \sqrt{\left(\frac{\Delta N_1}{N_1}\right)^2 + \left(\frac{\Delta N_2}{N_2}\right)^2 + \left(\frac{\Delta \frac{d\sigma_1}{d\Omega}}{\frac{d\sigma_1}{d\Omega}}\right)^2 + \left(\frac{\Delta \frac{d\sigma_2}{d\Omega}}{\frac{d\sigma_2}{d\Omega}}\right)^2}.$$

5: **Step 3: Calculate Compositions**

$$C_{\text{gold}} = \frac{1}{1 + R_{\text{Ag/Au}} + R_{\text{Cu/Au}}}, \tag{24}$$

$$C_{\text{silver}} = \frac{1}{1 + R_{\text{Au/Ag}} + R_{\text{Cu/Ag}}},$$

$$C_{\text{copper}} = 1 - C_{\text{gold}} - C_{\text{silver}}.$$

6: Calculate uncertainties in compositions:

$$\Delta C_{\text{gold}} = C_{\text{gold}}^2 \cdot \sqrt{\Delta R_{\text{Ag/Au}}^2 + \Delta R_{\text{Cu/Au}}^2}.$$

$$\Delta C_{\text{silver}} = C_{\text{silver}}^2 \cdot \sqrt{\Delta R_{\text{Au/Ag}}^2 + \Delta R_{\text{Cu/Ag}}^2}.$$

$$\Delta C_{\text{copper}} = \sqrt{\Delta C_{\text{gold}}^2 + \Delta C_{\text{silver}}^2}.$$

7: **Step 4: Output Results**

- Cross-sections with uncertainties.
- Partial ratios with uncertainties.
- Compositions ($C_{\text{gold}}, C_{\text{silver}}, C_{\text{copper}}$) with uncertainties.

Compositions of Target

- **Gold Composition:** 79.28 ± 1.12%
- **Silver Composition:** 10.99 ± 0.65%
- **Copper Composition:** 9.73 ± 1.30%

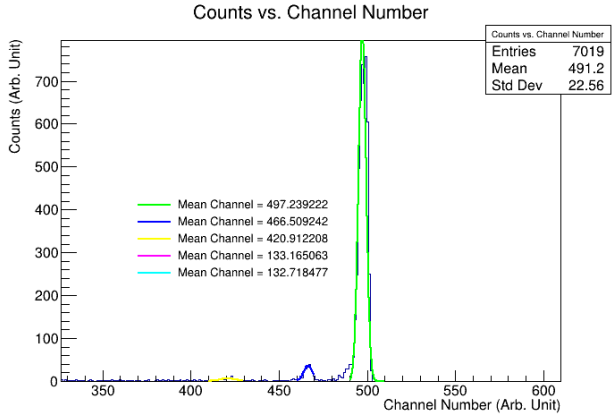

Figure 13: This is the resultant tag1061 file with the gold, silver and copper peaks displayed.

3.3 Theory Vs. Experiment

The goal of this step of the lab was to do one plot of the theoretical/experimental Rutherford's cross sections vs. an absolute scale of scattering angles (Detector angles). This plot is to see how close are the experimental and theoretical cross section data. Another test was to take experimental and theoretical values as divided ratios and plot that on this same angle scale to see a more concrete test of the fraction composed of the data. For example if the ratios on average converged to 1.0, then that would mean perfect agreement. The absolute scale of angles meant that all plots were plotted from the range of $0 \leq \theta_{sc} \leq 180$ degrees. All calculations used the given scattering angles for processing cross sections, but were converted to meet this absolute scale by applying a subtraction of 360 degrees then taken absolute if needed. Before more detail is given, an algorithm of calculating theoretical/experimental cross sections, finding ratios of cross sections, and getting uncertainties will be provided below. Now since algorithm is defined more detailed can be provided here: firstly the tags that were evaluated at this stage were the varying angles tags for RBS (ex. tag0031), the angles for the detector were used for calculating the theoretical differential cross sections, the dead time being corrected in decimal form, the target density was adjusted to account for gold contribution and thickness adjustment based of target angle orientation, and all steps applied unit conversions when necessary to eventually get to units of mb/sr. The comparison in general only was applied for the gold peaks. After all the necessary calculations were done the final step was to create the plots; to do that ROOT TGraphErrors class was also used in this step to do plotting. Based on figure 14, the theoretical and experimental curves generally had the same distributions with exception of angle ranges from $30 \leq \theta \leq 60$ degrees and this is because in the data collecting stages

those dead-times were incorrect. Also from figure 14, the ratio plot showed convergence within $R_{\text{Exp/theo}} = 0.7$. This shows only slight variation within most of the data which is approximate enough to say that experimental and theoretical Rutherford differential cross sections match. Table 2, are the the data values used for plotting comparisons. [Counts: 384]

Rutherford Cross Section Algorithm

Algorithm 3 Rutherford Gold Scattering Analysis

1: **Define Constants:**

$$\pi = 3.141592653589793 \quad \text{(Mathematical constant)}$$
$$E_0 = 2.5\,\text{MeV} \quad \text{(Initial energy of particles)}$$
$$Z_0 = 79.0 \quad \text{(Gold atomic number)}$$
$$Z_1 = 2.0 \quad \text{(Alpha particle atomic number)}$$
$$M_O = 4.002602\,\text{g/mol} \quad \text{(Mass of alpha particle)}$$
$$M_1 = 196.966570\,\text{g/mol} \quad \text{(Mass of gold atom)}$$
$$\rho = 8 \times 10^{17}\,\text{particles/cm}^2 \quad \text{(Target density)}$$
$$\text{cF} = 0.792819 \quad \text{(Gold composition fraction)}$$
$$\text{BCI} = 5000 \quad \text{(Beam Charge Intensity)}$$
$$R = 4.01\,\text{cm} \quad \Delta R = 0.035\,\text{cm (Uncertainty)}$$
$$r = 6.7\,\text{cm (Distance from detector to target)}$$

2: **Compute Solid Angle (Ω):**

$$A = \pi R^2 \quad \text{(Area of detector)}$$
$$\Delta A = 2\pi R \Delta R \quad \text{(Uncertainty in area)}$$
$$\Omega = \frac{A}{r^2} \quad \text{(Solid angle)}$$
$$\Delta\Omega = \Omega\sqrt{\left(\frac{\Delta A}{A}\right)^2} \quad \text{(Uncertainty in solid angle)}$$

3: **Initialize Variables:**

- θ: List of scattering (Detector) angles in degrees.
- N_s: Detected counts at each angle.
- DTL: Dead time losses (percentage).

Algorithm 4 Analysis Continued (Compact Version, Part 1)

for each angle θ_i in θ **do**

Step 1: Adjust Angles (For Plotting Only):

$$\theta_{\text{adjusted}} = \begin{cases} \theta_i - 360 & \text{if } \theta_i > 180, \\ \theta_i & \text{otherwise.} \end{cases}$$

Step 2: Theoretical Differential Cross-Section:

$$\frac{d\sigma}{d\Omega} = k \cdot \left(\frac{(Z_0 Z_1)^2}{E_0} \right)^2 \cdot \left(\frac{1}{\sin^4\left(\frac{\theta}{2}\right)} - 2 \cdot \frac{M_O^2}{M_1^2} \right)$$

Step 3: Uncertainty in $\frac{d\sigma}{d\Omega}$:

$$\Delta\left(\frac{d\sigma}{d\Omega}\right) = \sqrt{\left(\frac{\partial(d\sigma/d\Omega)}{\partial M_O} \Delta M_O \right)^2 + \left(\frac{\partial(d\sigma/d\Omega)}{\partial M_1} \Delta M_1 \right)^2}$$

Step 4: Corrected Counts (N_{corr}):

$$N_{\text{corr}} = \frac{N_s}{1 - \frac{\text{DTL}}{100}}$$

end for

Algorithm 5 Analysis Continued (Compact Version, Part 2)

for each angle θ_i in θ (continued) **do**

Step 5: Initial Alpha Particles (N_i):

$$N_i = \frac{\text{BCI} \cdot \text{Scale}}{Z \cdot e}, \quad \Delta N_i = \sqrt{N_i}$$

Step 6: Experimental Differential Cross-Section:

$$\frac{d\sigma_{\text{exp}}}{d\Omega} = \frac{N_{\text{corr}}}{\Omega \cdot N_i \cdot \rho_{\text{gold;adj}}}$$

Step 7: Uncertainty in $\frac{d\sigma_{\text{exp}}}{d\Omega}$:

$$\Delta\left(\frac{d\sigma_{\text{exp}}}{d\Omega}\right) = \frac{d\sigma_{\text{exp}}}{d\Omega}\sqrt{\left(\frac{\Delta N_{\text{corr}}}{N_{\text{corr}}}\right)^2 + \left(\frac{\Delta N_i}{N_i}\right)^2 + \left(\frac{\Delta\Omega}{\Omega}\right)^2}$$

Step 8: Ratio (R) and Its Uncertainty:

$$R = \frac{\frac{d\sigma_{\text{exp}}}{d\Omega}}{\frac{d\sigma}{d\Omega}}, \quad \Delta R = R\sqrt{\left(\frac{\Delta\left(\frac{d\sigma_{\text{exp}}}{d\Omega}\right)}{\frac{d\sigma_{\text{exp}}}{d\Omega}}\right)^2 + \left(\frac{\Delta\left(\frac{d\sigma}{d\Omega}\right)}{\frac{d\sigma}{d\Omega}}\right)^2}$$

end for

Plot Results:

- Plot $\frac{d\sigma}{d\Omega}$ (theoretical) vs. θ_{adjusted}.
- Plot $\frac{d\sigma_{\text{exp}}}{d\Omega}$ (experimental) vs. θ_{adjusted}.
- Combine theoretical and experimental plots into a single graph.
- Plot R vs. θ_{adjusted} on a separate canvas.

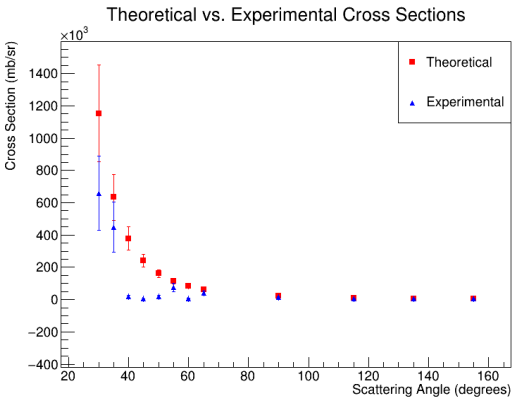

(a) Plot combined for the theoretical and experimental Rutherford differential cross section per adjusted angle.

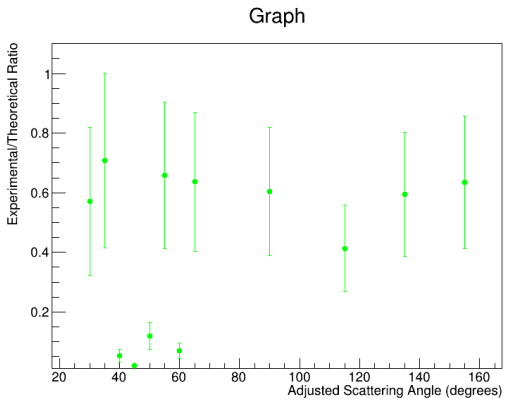

(b) Plot for the Rutherford differential cross section ratios per adjusted angle.

Figure 14: Display of all cross section data, that shows varying agreement with exception from ranges of $30 \leq \theta \leq 60$ degrees.

Differential Cross Sections and Ratios Data

Tag Number	$\frac{d\sigma_{\text{theo}}}{d\Omega}$ (mb/sr)	$\frac{d\sigma_{\text{exp}}}{d\Omega}$ (mb/sr)	$R = \frac{\frac{d\sigma_{\text{exp}}}{d\Omega}}{\frac{d\sigma_{\text{theo}}}{d\Omega}}$
21	5698.0 ± 88.6	3619 ± 1265	0.635 ± 0.222
31	82820 ± 10015	5760 ± 2012	0.0695 ± 0.0257
41	162269 ± 24295	19216 ± 6713	0.118 ± 0.045
51	378292 ± 72561	20179 ± 7049	0.0533 ± 0.0213
61	241364 ± 40681	4719.9 ± 1649.2	0.0196 ± 0.0076
71	113868 ± 15271	74889 ± 26160	0.658 ± 0.246
81	62107 ± 6806	39528 ± 13808	0.636 ± 0.233
91	20702 ± 1446	12517 ± 4372	0.605 ± 0.215
101	10227 ± 455	4228 ± 1477	0.413 ± 0.146
111	7101 ± 205	4215 ± 1473	0.594 ± 0.208
121	633095 ± 140180	448482 ± 156663	0.708 ± 0.293
131	1153590 ± 300566	657537 ± 229687	0.570 ± 0.248

Table 2: Theoretical and Experimental Differential Cross Sections (mb/sr) and Ratios for 13 Tags of varying angle.

4 Conclusion

This lab was done to introduce the ideas of Rutherford's Scattering to the accelerator lab here in Ohio University and to see how it could compare to theoretical predictions. To reiterate the tasks that were completed were calibration, Composition confirmation of the target, and theoretical/experimental cross section comparisons. For calibration it was done successfully because of residuals ranging from $-0.1 \leq R \leq 0.1$ Mev, the residuals plot converging to constant line, and to be able to find less prominent copper/silver peaks from tag 1061. For compositions they approximately matched the 80 %, 10 %, and 10% requirement for gold, silver and copper. The comparisons for both experimental and theoretical plots had same distribution with exception of angle ranges from $30 \leq \theta_{sc} \leq 60$ degrees because of dead-times values being incorrect. The ratio plots of cross sections converged approximately to $R = 0.7$, which shows close approximation of theoretical and experimental cross sections. The only thing that could be improved from this report is to have longer run times, and to see how the dead-times for those angle ranges were incorrect. [Counts: 183]

Works Cited

[1] Dr. Paul King. *Physics 6751: Nuclear Lab Manual*. Version 24.5. Athens, Ohio, 2024.

[2] John R. Taylor. *Classical Mechanics*. Collisions, Central Force Problem. Sausalito, CA: University Science Books, 2005. Chap. 14, 8.

[3] Nouredine Zettili. *Quantum Mechanics: Concepts and Applications*. 2nd. Scattering Theory. Wiley, 2009. Chap. 11.

[4] Ryan Conaway and Unish Gautam. *Rutherford: Lab Notes*. Lab Notes. Published on November 7, 2024. 2024. URL: N/A.

[5] Zach Meisel et al. "The Edwards Accelerator Laboratory at Ohio University". In: *Physics Procedia* 90 (2017). Presented at the Conference on the Application of Accelerators in Research and Industry (CAARI 2016), Ft. Worth, TX, USA., pp. 448–454. DOI: 10.1016/j.phpro.2017.09.050.

[6] National Institute of Standards and Technology (NIST). *Stopping-Power and Range Tables for Electrons, Protons, and Helium Ions (ASTAR)*. Accessed: 2024-11-27. 2024. URL: https://physics.nist.gov/PhysRefData/Star/Text/ASTAR.html.

[7] International Union of Pure and Applied Chemistry (IUPAC). *Standard Atomic Weights 2021*. Accessed: 2024-11-27. 2024. URL: https://iupac.qmul.ac.uk/AtWt/.

[8] National Center for Biotechnology Information (NCBI). *Helium: PubChem Element Summary*. Accessed: 2024-11-27. 2024. URL: https://pubchem.ncbi.nlm.nih.gov/element/2.